

## Interaction of casson nanofluid with Brownian motion: Temperature profile with shooting method

Waheed Iqbal<sup>1</sup>, Mudassar Jalil<sup>2</sup>, Mohamed A. Khadimallah<sup>3,4</sup>, Muzamal Hussain<sup>\*1</sup>,  
Muhammad N. Naeem<sup>1</sup>, Abdullah F. Al Naim<sup>5</sup> and Abdelouahed Tounsi<sup>6,7</sup>

<sup>1</sup> Department of Mathematics, Govt. College University Faisalabad, 38000, Faisalabad, Pakistan

<sup>2</sup> Department of Mathematics, COMSATS Institute of Information Technology, Park Road, Chak Shahzad, 44000 Islamabad, Pakistan

<sup>3</sup> Prince Sattam Bin Abdulaziz University, College of Engineering, Civil Engineering Department, BP 655, Al-Kharj, 16273, Saudi Arabia

<sup>4</sup> Laboratory of Systems and Applied Mechanics, Polytechnic School of Tunisia, University of Carthage, Tunis, Tunisia

<sup>5</sup> Department of Physics, College of Science, King Faisal University, P.O. Box 400, Al-Ahsa 31982, Saudi Arabia

<sup>6</sup> YFL (Yonsei Frontier Lab), Yonsei University, Seoul, Korea

<sup>7</sup> Department of Civil and Environmental Engineering, King Fahd University of Petroleum & Minerals,  
31261 Dhahran, Eastern Province, Saudi Arabia

(Received November 22, 2020, Revised December 5, 2020, Accepted December 8, 2020)

**Abstract.** In present study, the numerical investigations are carried out for effects of suction and blowing on boundary layer slip flow of casson nano fluid along permeable stretching cylinder in an exponential manner. The modeled PDEs are changed into nonlinear ODEs through appropriate nonlinear transformations. Change in physical quantities like friction coefficient, Nusselt and Sherwood numbers with variation of the aforementioned parameters are also examined and their numerical values are listed in the form of tables. Effects of Reynold number, suction parameter, Prandtl number, Lewis number, Brownian motion parameter and thermophoresis parameter are seen graphically with temperature profile.

**Keywords:** sherwood numbers; thermophoresis parameter; nonlinear ODEs; slip flow

### 1. Introduction

Casson fluids are blood, honey, plasma, Sauces etc. A lot of work has been done on study of Casson fluid flow over plate or flat surface; however, importance of research on flow of Casson fluid along other geometries is vital due to its various implementations in many industrial processes consisting of geometries like cylindrical shape. The main cause behind the immense interest of researchers is vast implementation of this phenomenon in lot of industrial and engineering processes for the sake of advancement in the techniques like manufacturing of metallic and plastic fiber sheets, making of copper wires, fabrication of electronic components, designing of water supply network and many more. Casson fluid is a form of Non-Newtonian fluid associated with yields stress.

In 1959, Casson proposed the model that was able to bear infinitely large viscosity without shear stress and conversely unlimited shear rate for zero viscosity. The detailed study of fluid flow along the stretched cylinder for the boundary layer was made (Ishak *et al.* 2009) regarding. Wang *et al.* (2011) obtained asymptotic solutions for high Reynold number using slip flow condition. Mixed convection condition together with slip flow and obtained

numerical solution for the boundary layer problem of Williamson fluid flow over a stretching cylinder (Salahuddin *et al.* 2017). The effects of Soret and Dufour for the Casson fluid by considering the heat transfer along stretching cylinder was worked out (Mahdy 2015). The mass and convective heat conditions for Casson fluid flow having nanoparticles along stretching cylinder was presented (Imtiaz *et al.* 2016a, b). A thorough numerical study of sisko fluid flow over stretching cylinder with effects of thermal conductivity and viscous dissipation was done (Malik *et al.* 2016). Al-Maliki *et al.* (2020) carried out the dynamic analysis of functionally graded (FG) graphene-reinforced beams under thermal loading based on finite element approach. The presented formulation is based on a higher order refined beam element accounting for shear deformations. The graphene-reinforced beam is exposed to transverse periodic mechanical loading. The uniform suction/blowing effects together with transfer of heat outside the permeable stretching cylinder were considered (Ishak *et al.* 2008). Under convective boundary conditions, electrically conducting sisko fluid along the stretching cylinder in axial direction was probed (Khan and Malik 2015). They found the considerable boost in the flow parameters for shear thinning than thickening. The notable point about all the above mentioned studies is that the considered fluid is "Pure". Practically it is almost impossible to have such fluid which is free from any kind of impurity. Every naturally occurring fluid contains dust particles. Many engineering and industrial problems deal with dusty fluid such as powder mechanization and

\*Corresponding author, Ph.D., Research Scholar,  
E-mail: muzamal45@gmail.com;  
muzamalhussain@gcuf.edu.pk

centrifugal technique to the detachment of particles from the fluid.

Flow of dusty fluid can be viewed in many natural phenomena e.g., flow of mud in rivers, blood flow and atmospheric flow during haze. Initiative study of motion of dust particles in laminar flow has been carried out (Saffman 1962). An analysis for viscous, incompressible steady flow of dusty fluid flowing between two co-axial rotating cylinders under pressure gradient effect was carried out (Nath 1970). Akgoz and Civalek (2011) investigated geometrically the nonlinear free vibration analysis of thin laminated plates resting on non-linear elastic foundations. Winkler-Pasternak type foundation model is used. Governing equations of motions are obtained using the von Karman type nonlinear theory. The method of discrete singular convolution is used to obtain the discretised equations of motion of plates. Akbaş (2018a, b, c) analyzed the objective of large deflections of a fiber reinforced composite cantilever beam under point loads. In the solution of the problem, finite element method is used in conjunction with two dimensional (2-D) continuum model. It is known that large deflection problems are geometrically nonlinear problems. In the nonlinear model of the laminated beam, total Lagrangian finite element model of is used in conjunction with the Timoshenko beam theory.

Batou *et al.* (2019) studied the wave propagations in sigmoid functionally graded (S-FG) plates using new Higher Shear Deformation Theory (HSST) based on two-dimensional (2D) elasticity theory. The current higher order theory has only four unknowns, which mean that few numbers of unknowns, compared with first shear deformations and others higher shear deformations theories and without needing shear corrector. Akbaş (2017a) investigated the free vibration analysis of edge cracked cantilever microscale beams composed of functionally graded material (FGM) ased on the modified couple stress theory (MCST). The material properties of the beam are assumed to change in the height direction according to the exponential distribution.

Baaskaran *et al.* (2018) studied the reliable and accurate method of computationally aided design processes of advanced thin walled structures in automotive industries for the efficient usage of smart materials, that possess higher energy absorption in dynamic compression loading. The most versatile components i.e., thin walled crash tubes with different geometrical profiles are introduced in view of mitigating the impact of varying cross section in crash behavior and energy absorption characteristics. A numerical scheme for the vibrating plate has been developed in the frame work of the higher-order mid-plane kinematics and the eigen frequencies are obtained by employing suitable finite element steps. Dusty gas flow in a region occupied by boundary layer was examined (Chakrabarti 1974). Akbaş (2020a) studied the dynamic responses of laminated composite beams under a moving load with thermal effects. The governing equations of problem are derived by using the Lagrange procedure. The transverse-shear strain and rotary inertia are considered within the Timoshenko beam theory. The material properties of laminas are considered as the temperature

dependent physical property.

The coefficient of friction and heat transfer for dusty boundary layer flow with pressure gradient was studied (Agranat 1988). In addition to these studies for flow and transfer of heat for dusty fluid along sheet / surface, many researchers considered dusty fluid flow along cylinder. The viscous, incompressible gas flow having dust particles for an isothermal cylinder was discussed and results from various physical parameters were presented (Rebhi 2010). Akbaş (2015) conducted the effect of material-temperature dependent on the wave propagation of a cantilever beam composed of functionally graded material (FGM) under the effect of an impact force. The beam is excited by a transverse triangular force impulse modulated by a harmonic motion. Material properties of the beam are temperature-dependent and change in the thickness direction. Chen *et al.* (2019) carried the energy absorption characteristics of a lattice-web reinforced composite sandwich cylinder (LRCSC) which is composed of glass fiber reinforced polymer (GFRP) face sheets, GFRP lattice webs, polyurethane (PU) foam and ceramsite filler. The vortex-induced vibration of three circular cylinders (each of diameter  $D$ ) in an equilateral triangular arrangement is investigated using the immersed boundary method. Abdulrazzaq *et al.* (2020) investigated the thermo-elastic buckling of small scale functionally graded material (FGM) nano-size plates with clamped edge conditions rested on an elastic substrate exposed to uniformly, linearly and non-linearly temperature distributions employing a secant function based refined theory. Material properties of the FGM nano-size plate have exponential gradation across the plate thickness. Akbaş (2020b) studied the axially damped forced vibration responses of viscoelastic nanorods within the frame of the modal analysis. The nonlocal elasticity theory is used in the constitutive relation of the nanorod with the Kelvin-Voigt viscoelastic model. In the forced vibration problem, a cantilever nanorod subjected to a harmonic load at the free end of the nanorod is considered in the numerical examples. Civalek (2017) investigated the free vibration analysis of conical and cylindrical shells and annular plates made of composite laminated and functionally graded materials (FGMs). Carbon nanotubes reinforced (CNTR) composite case is also taken consideration for FGM. The equations of motion for conical shell are obtained via Hamilton's principle using the transverse shear deformation theory. Some valuable results regarding heat transfer of dusty fluid over a hollow stretching cylinder using multi-step DTM were reported. Conduction of dusty fluid flow along stretching cylinder with thermal conductivity and viscosity effects were dealt numerically (Konch and Hazarika 2017). Turkyilmazoglu (2011) presented the impacts of thermal radiation on the unsteady laminar convective MHD flow of a viscous electrically conducting fluid having a temperature-dependent viscosity over a rotating porous disk. The fluid is subjected to an external uniform magnetic field perpendicular to the plane of the disk.

Akbaş (2019a, b, c) investigated the geometrically nonlinear static analysis and post buckling of laminated composite beams under hygrothermal effect. The finite

element method is used within the first shear beam theory. Total Lagrangian approach is used nonlinear kinematic model. The geometrically nonlinear formulations are developed for the laminated beams with hygro-thermal effects. Fiber-reinforced laminated composites are frequently preferred in many engineering projects. With the development in production technology, the using of the fiber reinforced laminated composites has been increasing in engineering applications. In the production stage of the fiber-reinforced laminated composites, porosities could be occurred due to production or technical errors.

Derakhshandeh and Alam (2020) investigated the Reynolds number  $Re$  ( $= 50-200$ ) effects on the flows around a single cylinder and the two tandem (center-to-center spacing  $L^* = L/D = 4$ ) cylinders, each of a diameter  $D$ . Vorticity structures, Strouhal numbers, and time-mean and fluctuating forces are presented and discussed. Salah *et al.* (2019) employed a simple four-variable integral plate theory for examining the thermal buckling properties of functionally graded material (FGM) sandwich plates. The proposed kinematics considers integral terms which include the effect of transverse shear deformations. In some fresh attempts, the researchers have pondered over new dimensions of stretching i.e., exponentially stretching cylinder. The detailed study of flow and transfer of heat for hyperbolic tangent fluid over a stretching cylinder exponentially in vertical direction was carried out (Naseer *et al.* 2014). Turkyilmazoglu (2016) considered the time-dependent flow past an impulsively started vertical infinite isothermal plate in a viscous electrically conducting natural convective incompressible nanofluid in this paper by taking into account the effects of heat absorption, heat generation, and radiation. Shadravan *et al.* (2019) performed lateral load testing on seventeen wood wall frames in two sections. Section one included eight tests studying structural foam sheathing of shear walls subjected to monotonic loads following the ASTM E564 test method. Turkyilmazoglu (2020) conducted the background and objective. The hydrodynamic stability of nanofluids of one phase based on linear stability theory. The overall thrust here is that the linear stability features of nanofluids can be estimated from their corresponding working fluid, at least in special circumstances.

Similarity solution has been derived for steady boundary layer and heat flow of Casson nanofluid (Malik *et al.* 2013) while cylinder was stretching exponentially along its radius. The flow of Micropolar fluid through vertical exponentially stretching cylinder along the axial direction and discussed heat transfer effects, too, were considered (Rehman 2015). Williamson fluid flow along an exponentially stretching cylinder was examined and they found its numerical solution (Iqbal *et al.* 2019). Recently some researcher used different methods for nonlinear modeling (Avcar 2019, Karami *et al.* 2018, Madani *et al.* 2016, Simsek 2011) and some other methods as open see software (Moghaddam and Masoodi 2019), first order shear deformation theory (Loghman *et al.* 2018), MLPG method (Rad *et al.* 2020), Ritz-type variational method (Sofiyev *et al.* 2006), Multiphysical numerical (FE-BE) solution and higher-order shear theory (Sharma and Panda 2020) and for nonlinear

modeling (Eltaher *et al.* 2019, Ebrahimi *et al.* 2019, Safaei *et al.* 2019, Shahsavari *et al.* 2019, Benmansour *et al.* 2019), Newton-Raphson iteration method, (Akbas 2017b, 2018c, d), Hamilton procedure (Akbas 2019d). All the above mentioned research work provides strong motivation for the present manuscript. In this paper, the effect of suction/blowing on boundary layer flow of Casson nanofluid along an exponentially stretching cylinder is examined and no such type of study is claimed till now. The influence of Reynold number ( $Re$ ), suction parameter ( $\kappa$ ), Prandtl number ( $Pr$ ), Lewis number ( $Le$ ), Brownian motion parameter ( $N_b$ ), of thermophoresis parameter ( $N_t$ ) on temperature profile.

## 2. Theoretical formation

The cylinder is stretching exponentially along positive  $z$ -axis with velocity  $U_w = 2ace^{z/a}$ , where  $c$  is the stretching rate. The origin stationary cylindrical coordinate system has positioned in the middle of the cylinder's leading edge, the  $z$ -axis is taken along axis of cylinder and  $r$ -axis is assumed in direction of radius of cylinder. Consider laminar, steady, viscous, incompressible boundary layer flow of Casson nanofluid at rest along a stretching cylinder of radius  $a$ . It is assumed that surface of cylinder has temperature  $T_w$  and ambient fluid temperature is  $T_\infty$ . It is also assumed that  $C_w$  is concentration of nanoparticles at the surface and  $C_\infty$  is ambient concentration. The viscous dissipation is neglected as it is assumed to be small. Under these assumptions, the governing equations of motion heat transfer and nano particle concentration are

$$\frac{\partial(ru)}{\partial z} + \frac{\partial(rv)}{\partial r} = 0, \quad \epsilon \leftrightarrow \epsilon \quad (1)$$

$$u \frac{\partial u}{\partial z} + v \frac{\partial u}{\partial r} = \nu \left(1 + \frac{1}{\beta}\right) \left(\frac{\partial^2 u}{\partial r^2} + \frac{1}{r} \frac{\partial u}{\partial r}\right) \quad (2)$$

$$u \frac{\partial T}{\partial z} + v \frac{\partial T}{\partial r} = \alpha \left(\frac{\partial^2 T}{\partial r^2} + \frac{1}{r} \frac{\partial T}{\partial r}\right) + \tau \left(D_B \frac{\partial T}{\partial r} \frac{\partial C}{\partial r} + \frac{D_T}{T_\infty} \left(\frac{\partial T}{\partial r}\right)^2\right) \quad (3)$$

$$u \frac{\partial C}{\partial z} + v \frac{\partial C}{\partial r} = D_B \left(\frac{\partial^2 C}{\partial r^2} + \frac{1}{r} \frac{\partial C}{\partial r}\right) + \frac{D_T}{T_\infty} \left(\frac{\partial^2 T}{\partial r^2} + \frac{1}{r} \frac{\partial T}{\partial r}\right) \quad (4)$$

$$\begin{aligned} r = a; \quad u = U_w + \frac{ay}{2} \frac{\partial u}{\partial r}, \\ v = V_w, \quad T = T_w = T_\infty + Ae^{(z/a)}, \\ C = C_w = C_\infty + Be^{(z/a)} \\ r \rightarrow \infty; \quad u = 0, \quad T \rightarrow T_\infty, \quad C \rightarrow C_\infty. \end{aligned} \quad (5)$$

Where  $(u, v)$  are the components of velocity of fluid respectively in  $(r, z)$  directions and  $T$  is the temperature.  $\nu$  denotes kinematic viscosity, thermal diffusivity represented

by  $\alpha$  of the fluid,  $\beta$  is used for the coefficient of thermal expansion,  $\tau$  ( $= (\rho c)_p/(\rho c)_f$ ) is the ratio of the effective heat capacity of the nanoparticle material to the effective heat capacity of the base fluid,  $C$  elaborates the nanoparticle Casson fluid concentration,  $D_B$  shows the Brownian diffusion coefficient, thermophoretic diffusion coefficient indicated by  $D_T$  and  $\gamma$  indicates velocity slip. Here  $V_w = -ac\kappa e^{z/a}$ , is suction velocity with  $\kappa > 0$  corresponds to mass suction and  $\kappa < 0$  indicates mass injection.

Eqs. (1)-(5) are non-linear coupled PDEs. These equations can easily be transformed into set of ODEs by using nonlinear transformations.

$$\zeta = \left(\frac{r}{a}\right)^2, \quad v = -\frac{1}{2}U_w \frac{g(\zeta)}{\sqrt{\zeta}}, \quad u = U_w g'(\zeta), \quad (6)$$

$$\theta(\zeta) = \frac{T - T_\infty}{T_w - T_\infty}, \quad \phi(\zeta) = \frac{C - C_\infty}{C_w - C_\infty}, \quad (7)$$

Where prime exhibits differentiation concerning ' $\zeta$ '. By using the above nonlinear transformation Eqs. (1) and (5) are transformed as

$$\zeta\theta'' + \theta' + Pr\{Re(g\theta' - g'\theta) + N_b\zeta\theta'\phi' + N_t\zeta\theta'^2\} = 0, \quad (8)$$

$$\zeta\phi'' + \phi' + Le Re(g\phi' - g'\phi) + \frac{N_t}{N_b}(\zeta\theta'' + \theta') = 0, \quad (9)$$

$$\begin{aligned} g(1) &= \kappa, & g'(1) &= 1 + \gamma g'', & g'(\infty) &= 0 \\ \theta(1) &= 1, & \theta(\infty) &= 0, & \phi(1) &= 1, & \phi(\infty) &= 0. \end{aligned} \quad (10)$$

where the non-dimensional parameters  $Re$ ,  $Pr$ ,  $N_b$  and  $N_t$  are defined as

$$\begin{aligned} Re &= \frac{aU_w}{4\nu}, & Pr &= \frac{\nu}{\alpha}, & Le &= \frac{\nu}{D_B}, \\ N_b &= \frac{\tau D_B (C_w - C_\infty)}{\nu}, & N_t &= \frac{\tau D_T (T_w - T_\infty)}{\nu T_\infty} \end{aligned} \quad (11)$$

Here  $Re$  denotes Reynolds number, Prandtl number represented by  $Pr$ ,  $Le$  indicates the Lewis number, Brownian motion parameter symbol used is  $N_b$  while  $N_t$  represents the thermophoresis parameter.

Physical quantities expressed by  $C_f$ ,  $Nu$  &  $Sh$  indicate the skin friction coefficient, Nusselt & Sherwood numbers, respectively and defined as

$$C_f = \frac{-\tau_w}{\rho U_w^2 / 2} \quad (12)$$

$$Nu = \frac{aq_w}{k(T_w - T_\infty)} \quad (13)$$

$$Sh = \frac{aq_m}{D_B(C_w - C_\infty)} \quad (14)$$

Where  $\tau_w$ ,  $q_w$  &  $q_m$  are the shear stress, rate of heat transfer & rate of mass transfer, respectively. These quantities are defined by

$$\tau_w = \mu \left(\frac{\partial u}{\partial r}\right) \Big|_{r=a} \quad (15)$$

$$q_w = -k \left(\frac{\partial T}{\partial r}\right) \Big|_{r=a} \quad (16)$$

$$q_m = -D_B \left(\frac{\partial C}{\partial r}\right) \Big|_{r=a} \quad (17)$$

Using the dimensionless transformation (6) in Eqs. (15)-(17) and substituting it in Eqs. (12)-(14), the dimensionless skin friction coefficient, Nusselt number and Sherwood number are achieved like

$$C_f Re = -g''(1) \quad (18)$$

$$Nu = -2\theta'(1) \quad (19)$$

$$Sh = -2\phi'(1) \quad (20)$$

Eqs. (7)-(10) are non-linear coupled ordinary differential equations. Exact analytical solution of these equations is not possible; therefore in the coming section numerical results of the problem are discussed and presented.

### 3. Results and discussion

The transformed nonlinear coupled ordinary differential equations are numerically solved using shooting method with RK-6 and findings are compared with the published work. For very large coefficient of thermal expansion ( $\beta$ ), the momentum equations of Casson nanofluid behaves like viscous fluid. Therefore, the results of coupled nonlinear ODE for Casson nanofluid must match to the results of coupled nonlinear ODE for viscous fluid. Current exertion is executed to discuss the flow behavior beneath the impact of several flow parameters for Casson nano fluid along a permeable cylinder that is stretching in an exponential way. Keeping view of such fluid behavior, the results of current problem, for the issue of no slip ( $\gamma = 0$ ) and very large  $\beta = 3000$ , are compared to the published results of similar equation for viscous fluid. In case of no slip ( $\gamma = 0$ ) and for very large  $\beta$  ( $\beta = 3000$ ), the nonlinear Eq. (7) becomes

$$(\zeta g''' + g'') + Re(gg'' - g'^2) = 0 \quad (21)$$

$$\begin{aligned} \zeta\phi'' + \phi' + Le Re(g\phi' - g'\phi) \\ + \frac{N_t}{N_b}(\zeta\theta'' + \theta') = 0, \end{aligned} \quad (22)$$

And the endpoint conditions of Eq. (10) takes the form

$$g(1) = \kappa, \quad g'(1) = 1, \quad g'(\infty) = 0 \quad (23)$$

The results of Eqs. (21) and (22) are presented by Ishak et al. (2008) and Wang and Ng (2011) for permeable and impermeable cases, respectively. In Table 1, a comparison is shown between our findings and the outcomes given by Ishak et al. (2008) and Wang and Ng (2011). An excellent agreement is noticed between the results which authenticates

Table 1 Comparison of values of  $-f''(1)$  with Wang and Ng (2011) for different values of Re and  $\kappa$

Re	$\kappa = 0$	
	Wang and Ng (2011)	Present
0.5	0.88220	0.882244
1	1.17776	1.177751
2	1.59390	1.593945
5	2.41745	2.417458
10	3.34445	3.344430

Table 2 Comparison of values of  $-f''(1)$  with Ishak *et al.* (2008) for different values of Re and  $\kappa$

Re	$\kappa = 0$	
	Ishak <i>et al.</i> (2008)	Present
0.5	1.0084	1.008201
1	1.4400	1.440175
2	2.1468	2.146859
5	3.9308	3.930836
10	6.6222	6.619664

the exactness of the procedure. Results are plotted both for suction ( $k = 0.5$ ) case. Current part deals with influential conduct of various parameters on velocity, temperature & mass concentration dimensionless distributions. Behavior of

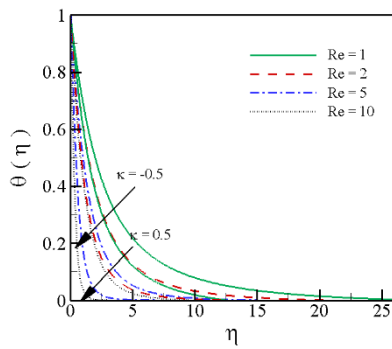


Fig. 1 Effects of Reynold number (Re) on temperature profile

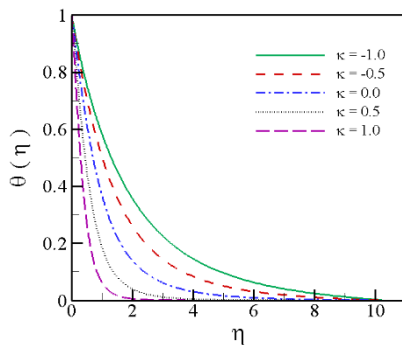


Fig. 2 Effects of suction parameter ( $\kappa$ ) on temperature profile

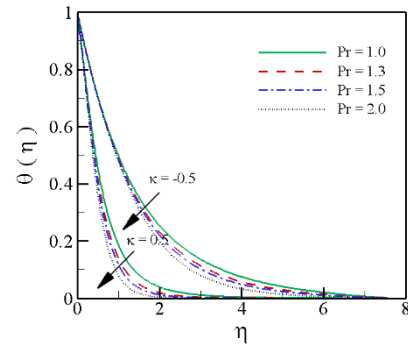


Fig. 3 Effects of Prandtl number (Pr) on temperature profile

Reynolds number on temperature profile is depicted in Fig. 1. Considerable reduction in fluid temperature is noticed due to amplification of fluid viscosity with rise of  $Re$  and consequently thermal boundary layer becomes thin. An obvious drop in fluid temperature is seen in Fig. 2 with expansion of suction parameter ( $k$ ). High suction generates resistance at stretching boundary and thins thermal boundary layer.

Fig. 3 reveals impact of prandtl number on temperature field. Higher values of prandtl number cools down the fluid. As thermal diffusivity is inversely related to  $Pr$ , so rapid diffusion of heat takes place for large prandtl number. Fig. 4 is framed for the variation of Lewis number ( $Le$ ) on temperature of fluid demonstration. According to definition ratio of thermal diffusion to mass diffusion stands for  $Le$ . Therefore, fluid temperature drops down for growing values of Lewis number. Fig. 5 interprets Brownian motion

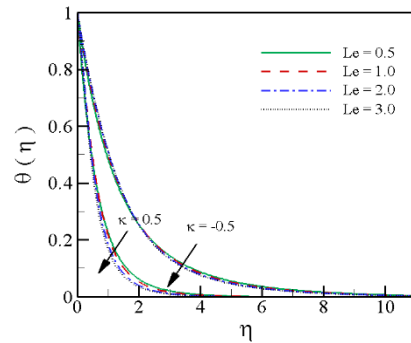


Fig. 4 Effects of Lewis number ( $Le$ ) on temperature profile

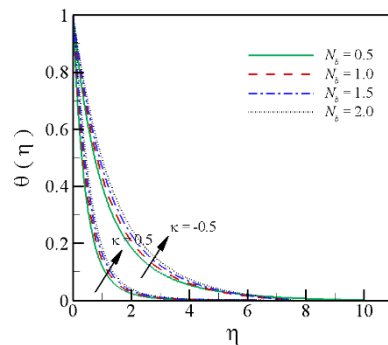


Fig. 5 Effects of Brownian motion parameter ( $N_b$ ) on temperature profile

influence on fluid temperature. A rise in temperature is happened due to strong Brownian motion of nano particles. Enhancement in  $N_b$ , produces the rapid movements of fluid particles and, in turns, the kinetic energy is remarkably

increased. Due to the direct linkage of  $K.E$  and temperature intensify the temperature of fluid.

Fig. 6 is plotted for temperature field against thermospheres parameter ( $N_t$ ). Boost of fluid temperature is noted for large thermosteresis parameter. Since high  $N_t$  strengthen the thermopheretic force which shifts the nano particles from hot to cooler region. Due to this particular activity, fluid temperature climbs up. Along  $k = 0$  and  $k \neq 0$ , Numerical conclusion of Nusselt number ( $Nu$ ) for flow parameters  $\gamma, \beta, Re, Pr, Le, N_b$  and  $N_t$  are tabulated in Table 3. All the parameters dropped down the  $Nu$  for both permeable and impermeable surfaces Whereas  $Re$  is the only exception trending opposite.

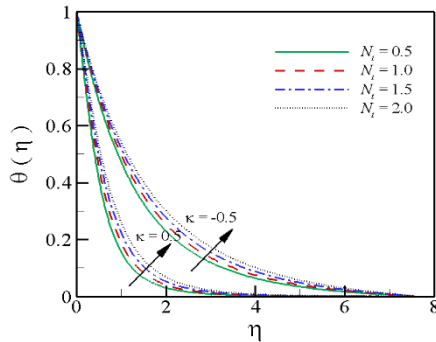


Fig. 6 Effects of thermophoresis parameter ( $N_t$ ) on temperature profile

### 4. Conclusions

In current study, numerical results are attained using a renowned numerical scheme shooting method with Runge-Kutta procedure of 6<sup>th</sup>-order. The special effects of Reynold

Table 3 Numerical results of Nusselt Number  $Nu$  for distinct values of  $\gamma, \beta, Re, Pr, Le, N_b$  and  $N_t$  with impermeable ( $\kappa = 0$ ) and permeable surfaces ( $\kappa \neq 0$ )

$\gamma$	$\beta$	Re	Pr	Le	$N_b$	$N_t$	Nu		
							$\kappa = 0$	$\kappa = -0.5$	$\kappa = 0.5$
0.1	2.0	5.0	1.0	1.0	2.0	1.0	1.8182	1.500596	2.388435
0.5							1.598437	1.304679	2.187075
1.0							1.448462	1.151306	2.052587
2.0							1.166043	1.010284	1.80848
0.2	0.1						1.901442	1.512783	2.497273
	0.4						1.806457	1.458703	2.384388
	0.7						1.766787	1.441365	2.294261
	1.0						1.744449	1.432335	2.249128
		1					0.827494	0.768544	0.926476
		2					1.138251	1.009364	1.348686
		5					1.767199	1.425089	2.341321
		10					2.322417	1.797064	3.600423
			1.0				1.707771	1.448552	2.285392
			1.3				1.686971	1.444809	2.252502
			1.5				1.667461	1.441766	2.209821
			2.0				1.615764	1.435912	2.080307
				0.5			2.122329	1.55366	2.85001
				1.0			1.742708	1.434908	2.094089
				2.0			1.425766	1.351656	1.521891
				3.0			1.272417	1.320705	1.285036
					0.5		2.884495	1.989162	4.705484
					1.0		2.396686	1.778908	3.697714
					1.5		2.002914	1.600769	2.896331
					2.0		1.68421	1.448552	2.266609
						0.5	1.841906	1.535316	2.513872
						1.0	1.698282	1.448552	2.266609
						1.5	1.579707	1.375691	2.066012
						2.0	1.48076	1.313752	1.900319

number ( $Re$ ), suction parameter ( $\kappa$ ), Prandtl number ( $Pr$ ), Lewis number ( $Le$ ), Brownian motion parameter ( $N_b$ ), and thermophoresis parameter ( $N_t$ ) are seen graphically with temperature profile. To ensure the authenticity of numerical procedure, outcomes of some special cases of present work are compared with published work and strong agreement is noticed. Demonstration of temperature distribution go upward for arising values of  $N_b$ ,  $N_t$ ,  $\beta$  and  $\gamma$ . The Reduction in temperature distribution have been seen for ascending values of  $Re$ ,  $Pr$ ,  $k$  &  $Le$ . The present studied cab be extended for the clamped exponentially graded shell according to a secant function based refined theory.

### Declaration of conflicting interests

The author(s) declared no potential conflicts of interest with respect to the research, authorship, and/or publication of this article.

### Acknowledgments

This project was supported by the Deanship of Scientific Research at Prince Sattam Bin Abdulaziz University under the research project No 16794/01/2020.

### ORCID iD

Muzamal Hussain

<http://orcid.org/0000-0002-6226-359X>

### References

- Abdulrazzaq, M.A., Fenjan, R.M., Ahmed, R.A. and Faleh, N.M. (2020), "Thermal buckling of nonlocal clamped exponentially graded plate according to a secant function based refined theory", *Steel Compos. Struct., Int. J.*, **35**(1), 147-57. <https://doi.org/10.12989/scs.2020.35.1.147>
- Agranat, V.M. (1988), "Effect of pressure gradient on friction and heat transfer in a dusty boundary layer", *Fluid Dyn.*, **23**, 729-732. <http://dx.doi.org/10.1007/BF02614150>
- Akbaş, Ş.D. (2015), "Wave propagation of a functionally graded beam in thermal environments", *Steel Compos. Struct., Int. J.*, **19**(6), 1421-1447. <https://doi.org/10.12989/scs.2015.19.6.1421>
- Akbaş, Ş.D. (2017a), "Free vibration of edge cracked functionally graded microscale beams based on the modified couple stress theory", *Int. J. Struct. Stabil. Dyn.*, **17**(3), 1750033. <https://doi.org/10.1142/S021945541750033X>
- Akbaş, Ş.D. (2017b), "Nonlinear static analysis of functionally graded porous beams under thermal effect", *Coupled Syst. Mech., Int. J.*, **6**(4), 399-415. <https://doi.org/10.12989/csm.2017.6.4.399>
- Akbaş, S.D. (2018a), "Large deflection analysis of a fiber reinforced composite beam", *Steel Compos. Struct., Int. J.*, **27**(5), 567-576. <https://doi.org/10.12989/scs.2018.27.5.567>
- Akbaş, S.D. (2018b), "Geometrically nonlinear analysis of a laminated composite beam", *Struct. Eng. Mech., Int. J.*, **66**(1), 27-36. <https://doi.org/10.12989/sem.2018.66.1.027>
- Akbaş, S.D. (2018c), "Post-buckling responses of a laminated composite beam", *Steel Compos. Struct., Int. J.*, **26**(6), 733-743. <https://doi.org/10.12989/scs.2018.26.6.733>
- Akbaş, Ş.D. (2018d), "Thermal post-buckling analysis of a laminated composite beam", *Struct. Eng. Mech., Int. J.*, **67**(4), 337-346. <https://doi.org/10.12989/sem.2018.67.4.337>
- Akbaş, Ş.D. (2018e), "Nonlinear thermal displacements of laminated composite beams", *Coupled Syst. Mech., Int. J.*, **7**(6), 691-705. <https://doi.org/10.12989/csm.2018.7.6.691>
- Akbaş, Ş.D. (2019a), "Nonlinear static analysis of laminated composite beams under hygro-thermal effect", *Struct. Eng. Mech., Int. J.*, **72**(4), 433-441. <https://doi.org/10.12989/sem.2019.72.4.433>
- Akbaş, Ş.D. (2019b), "Post-buckling analysis of a fiber reinforced composite beam with crack", *Eng. Fract. Mech.*, **212**, 70-80. <https://doi.org/10.1016/j.engfracmech.2019.03.007>
- Akbaş, Ş.D. (2019c), "Hygrothermal post-buckling analysis of laminated composite beams", *Int. J. Appl. Mech.*, **11**(1), 1950009. <https://doi.org/10.1142/S1758825119500091>
- Akbaş, Ş.D. (2019d), "Forced vibration analysis of functionally graded sandwich deep beams", *Coupled Syst. Mech., Int. J.*, **8**(3), 259-271. <https://doi.org/10.12989/csm.2019.8.3.259>
- Akbaş, Ş.D. (2020a), "Dynamic responses of laminated beams under a moving load in thermal environment", *Steel Compos. Struct., Int. J.*, **35**(6), 729-737. <https://doi.org/10.12989/scs.2020.35.6.729>
- Akbaş, Ş.D. (2020b), "Modal analysis of viscoelastic nanorods under an axially harmonic load", *Adv. Nano Res., Int. J.*, **8**(4), 277-282. <https://doi.org/10.12989/anr.2020.8.4.277>
- Akgoz, B. and Civalek, O. (2011), "Nonlinear vibration analysis of laminated plates resting on nonlinear two-parameters elastic foundations", *Steel Compos. Struct., Int. J.*, **11**(5), 403-421. <https://doi.org/10.12989/scs.2011.11.5.403>
- Al-Maliki, A.F., Ahmed, R.A., Moustafa, N.M. and Faleh, N.M. (2020), "Finite element based modeling and thermal dynamic analysis of functionally graded graphene reinforced beams", *Adv. Computat. Des., Int. J.*, **5**(2), 177-193. <https://doi.org/10.12989/acd.2020.5.2.177>
- Avcar, M. (2019), "Free vibration of imperfect sigmoid and power law functionally graded beams", *Steel Compos. Struct., Int. J.*, **30**(6), 603-615. <https://doi.org/10.12989/scs.2019.30.6.603>
- Baaskaran, N., Ponappa, K. and Shankar, S. (2018), "Assessment of dynamic crushing and energy absorption characteristics of thin-walled cylinders due to axial and oblique impact load", *Steel Compos. Struct., Int. J.*, **28**(2), 179-194. <https://doi.org/10.12989/scs.2018.28.2.179>
- Batou, B., Nebab, M., Bennai, R., Atmane, H.A., Tounsi, A. and Bouremana, M. (2019), "Wave dispersion properties in imperfect sigmoid plates using various HSDTs", *Steel Compos. Struct., Int. J.*, **33**(5), 699-716. <https://doi.org/10.12989/scs.2019.33.5.699>
- Benmansour, D.L., Kaci, A., Bousahla, A.A., Heireche, H., Tounsi, A., Alwabri, A.S., Alhebshi, A.M., Al-ghmady, K. and Mahmoud, S.R. (2019), "The nano scale bending and dynamic properties of isolated protein microtubules based on modified strain gradient theory", *Adv. Nano Res., Int. J.*, **7**(6), 443-457. <https://doi.org/10.12989/anr.2019.7.6.443>
- Chakrabarti, K.M. (1974), "Note on Boundary layer in a dusty gas", *Am. Inst. Aeronaut. Astronaut. J.*, **12**, 1136-1137. <http://dx.doi.org/10.2514/3.49427>
- Chen, J., Zhuang, Y., Fang, H., Liu, W., Zhu, L. and Fan, Z. (2019), "Energy absorption of foam-filled lattice composite cylinders under lateral compressive loading", *Steel Compos. Struct., Int. J.*, **31**(2), 133-148. <https://doi.org/10.12989/scs.2019.31.2.133>
- Civalek, Ö. (2017), "Free vibration of carbon nanotubes reinforced (CNTR) and functionally graded shells and plates based on FSDT via discrete singular convolution method", *Compos. Part B: Eng.*, **111**, 45-59.

- <https://doi.org/10.1016/j.compositesb.2016.11.030>
- Derakhshandeh, J.F. and Alam, M.M. (2020), "Reynolds number effect on the flow past two tandem cylinders", *Wind Struct., Int. J.*, **30**(5), 475-483. <https://doi.org/10.12989/was.2020.30.5.475>
- Ebrahimi, F., Dabbagh, A., Rabczuk, T. and Tornabene, F. (2019), "Analysis of propagation characteristics of elastic waves in heterogeneous nanobeams employing a new two-step porosity-dependent homogenization scheme", *Adv. Nano Res., Int. J.*, **7**(2), 135-143. <https://doi.org/10.12989/anr.2019.7.2.135>
- Eltaher, M.A., Almalki, T.A., Ahmed, K.I. and Almitani, K.H. (2019), "Characterization and behaviors of single walled carbon nanotube by equivalent-continuum mechanics approach", *Adv. Nano Res., Int. J.*, **7**(1), 39-49. <https://doi.org/10.12989/anr.2019.7.1.039>
- Iqbal, W., Naeem, M.N. and Jalil, M. (2019), "Numerical analysis of Williamson fluid flow along an exponentially stretching cylinder", *AIP Advances*, **9**(5), 055118. <http://dx.doi.org/10.1063/1.5092737>
- Ishak, A., Nazar, R. and Pop, I. (2008), "Uniform suction/ blowing effect on flow and heat transfer due to stretching cylinder", *App. Math. Mod.*, **32**, 2059-2066. <http://dx.doi.org/10.1016/j.apm.2007.06.036>
- Ishak, A., Nazar, R. and Pop, I. (2009), "Boundary layer flow and heat transfer over an unsteady stretching vertical surface", *Meccanica*, **44**(4), 369-375. <https://doi.org/10.1007/s11012-008-9176-9>
- Karami, B., Janghorban, M. and Tounsi, A. (2018), "Nonlocal strain gradient 3D elasticity theory for anisotropic spherical nanoparticles", *Steel Compos. Struct., Int. J.*, **27**(2), 201-216. <https://doi.org/10.12989/scs.2018.27.2.201>
- Khan, M. and Malik, R. (2015), "Forced convective heat transfer to Sisko fluid flow past a stretching cylinder", *AIP Advances*, **5**(12), 127202. <http://dx.doi.org/10.1063/1.4937346>
- Konch, J. and Hazarika, G.C. (2017), "Unsteady Hydro magnetic flow of dusty fluid over a stretching cylinder with variable viscosity and thermal conductivity", *Int. J. Adv. Sci. Tech.*, **99**, 57-70. <http://dx.doi.org/10.14257/ijast.2017.99.05>
- Imtiaz, M., Hayat, T. and Alsaedi, A. (2016a), "Mixed convection flow of Casson nanofluid over a stretching cylinder with convective boundary conditions", *Adv. Power Tech.*, **27**(5), 2245-2256. <https://doi.org/10.1016/j.appt.2016.08.011>
- Imtiaz, M., Hayat, T. and Alsaedi, A. (2016b), "MHD convective flow of Jeffrey fluid due to a curved stretching surface with homogeneous-heterogeneous reactions", *Plos one*, **11**(9), e0161641. <https://doi.org/10.1371/journal.pone.0161641>
- Iqbal, W., Naeem, M.N. and Jalil, M. (2019), "Numerical analysis of Williamson fluid flow along an exponentially stretching cylinder", *AIP Adv.*, **9**(5), 055118. <https://doi.org/10.1063/1.5092737>
- Ishak, A., Nazar, R. and Pop, I. (2008), "Hydromagnetic flow and heat transfer adjacent to a stretching vertical sheet", *Heat Mass Transfer*, **44**(8), 921-927. <https://doi.org/10.1007/s00231-007-0322-z>
- Loghman, A., Faegh, R.K. and Arefi, M. (2018), "Two dimensional time-dependent creep analysis of a thick-walled FG cylinder based on first order shear deformation theory", *Steel Compos. Struct., Int. J.*, **26**(5), 533-547. <https://doi.org/10.12989/scs.2018.26.5.533>
- Madani, H., Hosseini, H. and Shokravi, M. (2016), "Differential cubature method for vibration analysis of embedded FG-CNT-reinforced piezoelectric cylindrical shells subjected to uniform and non-uniform temperature distributions", *Steel Compos. Struct., Int. J.*, **22**(4), 889-913. <https://doi.org/10.12989/scs.2016.22.4.889>
- Mahdy, A. (2015), "Heat transfer and flow of a Casson fluid due to a stretching cylinder with the sores and dufour effects", *J. Eng. Phys. Thermophys.*, **88**(4), 928-936. <https://doi.org/10.1007/s10891-015-1267-6>
- Malik, M.Y., Naseer, M., Nadeem, S. and Rehman, A. (2013), "The boundary layer flow of Casson nanofluid over an exponentially stretching cylinder", *Appl. Nanosci.*, **4**, 869-873. <https://doi.org/10.1007/s13204-013-0267-0>
- Malik, M.Y., Hussain, A., Salahuddin, T., Awais, M., Bilal, S. and Khan, F. (2016), "Flow of Sisko fluid over a stretching cylinder and heat transfer with viscous dissipation and variable thermal conductivity: A numerical study", *AIP Advances*, **6**(4), 045118. <https://doi.org/10.1063/1.4948458>
- Moghaddam, S.H. and Masoodi, A.R. (2019), "Elastoplastic nonlinear behavior of planar steel gabled frame", *Adv. Computat. Des., Int. J.*, **4**(4), 397-413. <https://doi.org/10.12989/acd.2019.4.4.397>
- Naseer, M., Malik, M.Y., Nadeem, S. and Rehman, A. (2014), "The boundary layer flow of hyperbolic tangent fluid over a vertical exponentially stretching cylinder", *Alexandria Eng. J.*, **53**, 747-750. <https://doi.org/10.1016/j.aej.2014.05.001>
- Nath, G. (1970), "DUSTY VISCOUS-FLUID FLOW BETWEEN ROTATING COAXIAL CYLINDERS", *PROCEEDINGS OF THE NATIONAL ACADEMY OF SCIENCES INDIA SECTION A-PHYSICAL SCIENCES*, **40**(3), 257.
- Rad, M.H.G., Shahabian, F. and Hosseini, S.M. (2020), "Geometrically nonlinear dynamic analysis of FG graphene platelets-reinforced nanocomposite cylinder: MLPG method based on a modified nonlinear micromechanical model", *Steel Compos. Struct., Int. J.*, **35**(1), 77-92. <https://doi.org/10.12989/scs.2020.35.1.077>
- Rasekh, A., Ganji, D.D., Tavakoli, S., Ehsani, H. and Naejee, S. (2014), "MHD flow and heat transfer of dusty fluid over a stretching hollow cylinder with a convective boundary conditions", *Heat Trans. Asian Res.*, **43**(3), 221-232. <https://doi.org/10.1002/htj.21073>
- Rebhi, A.D. (2010), "On boundary layer flow of dusty gas from a horizontal circular cylinder", *Braz. J. Chem. Eng.*, **27**(4), 653-662. <http://dx.doi.org/10.1590/S0104-66322010000400017>
- Rehman, A. (2015), "Boundary layer flow and heat transfer of Micropolar Fluid over a vertical exponentially stretching cylinder", *Appl. Compos. Math.*, **4**(6), 424-430. <http://dx.doi.org/10.11648/j.acm.20150406.15>
- Safaei, B., Khoda, F.H. and Fattahi, A.M. (2019), "Non-classical plate model for single-layered graphene sheet for axial buckling", *Adv. Nano Res., Int. J.*, **7**(4), 265-275. <https://doi.org/10.12989/anr.2019.7.4.265>
- Saffman, P.G. (1962), "On the stability of laminar flow of a dusty gas", *J. Fluid Mech.*, **13**, 120-128. <https://doi.org/10.1017/S0022112062000555>
- Salah, F., Boucham, B., Bourada, F., Benzair, A., Bousahla, A.A. and Tounsi, A. (2019), "Investigation of thermal buckling properties of ceramic-metal FGM sandwich plates using 2D integral plate model", *Steel Compos. Struct., Int. J.*, **33**(6), 805-822. <https://doi.org/10.12989/scs.2019.33.6.805>
- Salahuddin, T., Malik, M.Y., Hussain, A., Awais, M. and Bilal, S. (2017), "Mixed convection boundary layer flow of Williamson fluid with slip conditions over a stretching cylinder by using Keller-box method", *Int. J. Nonlinear Sci. Numer. Simul.*, **18**(1), 9-17. <https://doi.org/10.1515/ijnsns.2015.0090>
- Shadravan, S., Ramseyer, C.C. and Floyd, R.W. (2019), "Comparison of structural foam sheathing and oriented strand board panels of shear walls under lateral load", *Adv. Computat. Des., Int. J.*, **4**(3), 251-272. <https://doi.org/10.12989/acd.2019.4.3.251>
- Shahsavari, D., Karami, B. and Janghorban, M. (2019), "Size-dependent vibration analysis of laminated composite plates", *Adv. Nano Res., Int. J.*, **7**(5), 337-349. <https://doi.org/10.12989/anr.2019.7.5.337>
- Sharma, N. and Panda, S.K. (2020), "Multiphysical numerical (FE-BE) solution of sound radiation responses of laminated

- sandwich shell panel including curvature effect”, *Comput. Mathe. Applicat.*, **80**(5), 1221-1239.  
<https://doi.org/10.1016/j.camwa.2020.06.010>
- Simsek, M. (2011), “Forced vibration of an embedded single-walled carbon nanotube traversed by a moving load using nonlocal Timoshenko beam theory”, *Steel Compos. Struct., Int. J.*, **11**(1), 59-76. <https://doi.org/10.12989/scs.2011.11.1.059>
- Sofiyev, A.H., Yücel, K., Avcar, M. and Zerir, Z. (2006), “The dynamic stability of orthotropic cylindrical shells with non-homogenous material properties under axial compressive load varying as a parabolic function of time”, *J. Reinf. Plastics Compos.*, **25**(18), 1877-1886.  
<https://doi.org/10.1177/0731684406069914>
- Turkyilmazoglu, M. (2011), “Thermal radiation effects on the time-dependent MHD permeable flow having variable viscosity”, *Int. J. Thermal Sci.*, **50**(1), 88-96.  
<https://doi.org/10.1016/j.ijthermalsci.2010.08.016>
- Turkyilmazoglu, M. (2016), “Natural convective flow of nanofluids past a radiative and impulsive vertical plate”, *J. Aerosp. Eng.*, **29**(6), 04016049.  
[https://doi.org/10.1061/\(ASCE\)AS.1943-5525.0000643](https://doi.org/10.1061/(ASCE)AS.1943-5525.0000643)
- Turkyilmazoglu, M. (2020), “Single phase nanofluids in fluid mechanics and their hydrodynamic linear stability analysis”, *Comput. Methods Programs Biomed.*, **187**, 105171.  
<https://doi.org/10.1016/j.cmpb.2019.105171>
- Wang, C.Y. and Ng, C-O. (2011), “Slip flow due to a stretching cylinder”, *Int. J. Non-Lin. Mech.*, **46**, 1191-1194.  
<https://doi.org/10.1016/j.ijnonlinmec.2011.05.04>
- Wang, L., Liu, J., Li, X., Shi, J., Hu, J., Cui, R., Zhang, Z.L., Pang, D.W. and Chen, Y. (2011), “Growth propagation of yeast in linear arrays of microfluidic chambers over many generations”, *Biomicrofluidics*, **5**(4), 044118.  
<https://doi.org/10.1063/1.3668243>
- Yüksel, Y.Z. and Akbaş, Ş.D. (2019), “Buckling analysis of a fiber reinforced laminated composite plate with porosity”, *J. Computat. Appl. Mech.*, **50**(2), 375-380.  
<https://doi.org/10.22059/JCAMECH.2019.291967.448>